

Host Prostaglandin E₂-EP3 Signaling Regulates Tumor-Associated Angiogenesis and Tumor Growth

Hideki Amano,^{1,2} Izumi Hayashi,¹ Hirahito Endo,³ Hidero Kitasato,⁴ Shohei Yamashina,⁵ Takayuki Maruyama,⁶ Michiyoshi Kobayashi,⁶ Kazutoyo Satoh,⁶ Masami Narita,⁶ Yukihiko Sugimoto,⁷ Takahiko Murata,⁸ Hirokuni Yoshimura,² Shuh Narumiya,⁸ and Masataka Majima¹

¹Department of Pharmacology, ²Department of Thoracic Surgery, ³Department of Internal Medicine, ⁴Department of Microbiology, and ⁵Department of Anatomy, Kitasato University School of Medicine, Kanagawa 228-8555, Japan
⁶Minase Research Institute, Ono Pharmaceutical Co. Ltd., Osaka 618-8585, Japan
⁷Department of Physiological Chemistry, Faculty of Pharmaceutical Sciences, and ⁸Department of Pharmacology, Faculty of Medicine, Kyoto University, Kyoto 606-8501, Japan

Abstract

Nonsteroidal antiinflammatories are known to suppress incidence and progression of malignancies including colorectal cancers. However, the precise mechanism of this action remains unknown. Using prostaglandin (PG) receptor knockout mice, we have evaluated a role of PGs in tumor-associated angiogenesis and tumor growth, and identified PG receptors involved. Sarcoma-180 cells implanted in wild-type (WT) mice formed a tumor with extensive angiogenesis, which was greatly suppressed by specific inhibitors for cyclooxygenase (COX)-2 but not for COX-1. Angiogenesis in sponge implantation model, which can mimic tumor-stromal angiogenesis, was markedly suppressed in mice lacking EP3 (EP3^{-/-}) with reduced expression of vascular endothelial growth factor (VEGF) around the sponge implants. Further, implanted tumor growth (sarcoma-180, Lewis lung carcinoma) was markedly suppressed in EP3^{-/-}, in which tumor-associated angiogenesis was also reduced. Immunohistochemical analysis revealed that major VEGF-expressing cells in the stroma were CD3/Mac-1 double-negative fibroblasts, and that VEGF-expression in the stroma was markedly reduced in EP3^{-/-}, compared with WT. Application of an EP3 receptor antagonist inhibited tumor growth and angiogenesis in WT, but not in EP3^{-/-}. These results demonstrate significance of host stromal PGE₂-EP3 receptor signaling in tumor development and angiogenesis. An EP3 receptor antagonist may be a candidate of chemopreventive agents effective for malignant tumors.

Key words: angiogenesis • tumor • prostaglandin E₂ • EP3 receptor • vascular endothelial growth factor

Introduction

Nonsteroidal antiinflammatory drugs (NSAIDs)* that inhibit the enzyme cyclooxygenase (COX) and suppress PG synthesis have been widely used as antiinflammatory, antipyretic, and analgesic agents. Recent epidemiological studies revealed a 40–50% reduction in mortality from colorectal cancer in individuals taking NSAIDs, and evidence suggests that they also affect the incidence and progression of other types of

cancer, pointing to a possible role of COX in tumor formation (1). PGs including PGE₂ and PGI₂ comprise a group of oxygenated metabolites of arachidonic acid that are produced by the sequential actions of cyclooxygenase (COX) and specific synthases. Two COX isoforms have been identified: COX-1 is constitutively expressed in various tissues, whereas COX-2 is induced by mitogens, cytokines, and tumor promoters. Disruption of the COX-2 gene in mice reduced the number and size of intestinal polyps generated by a mutation in the adenomatous polyposis (APC) gene, thus verifying a role for COX-2 in the generation of colon tumors (2). In spite of the efficacy of NSAIDs as anticancer agents, the precise mechanism(s) for the protective effect remain unknown. An intense debate is underway that focuses on a wide range of mechanisms of antitumor action of

H. Amano and I. Hayashi contributed equally to this work.

Address correspondence to Masataka Majima, Department of Pharmacology, Kitasato University School of Medicine, Kitasato 1-15-1, Sagami-hara, Kanagawa 228-8555, Japan. Phone: 81-42-778-8822; Fax: 81-42-778-7604; E-mail: en3m-mjm@asahi-net.or.jp

*Abbreviations used in this paper: COX, cyclooxygenase; NSAID, nonsteroidal antiinflammatory drugs.

NSAIDs, some of which are unrelated to inhibition of cyclooxygenase activity (3, 4, 5).

Angiogenesis is an important factor in tumor development, and tumor-associated angiogenesis is mediated by the migration and proliferation of host endothelial cells. With the use of a coculture system comprising endothelial cells and colon carcinoma cells that overexpress COX-2, Tsujii et al. (6) showed that the increased production of PGs by the carcinoma cells was associated with endothelial cell migration and tube formation, suggesting a role for COX-2 in tumor-induced angiogenesis. However, the relevance of these *in vitro* observations to tumorigenesis *in vivo* remains to be established. Furthermore, whether PGs actually contribute to the observed tumor-associated angiogenesis, and, if so, the identity of the responsible PGs and PG receptors, remains unknown.

For mechanistic analysis of angiogenesis *in vivo*, we have developed a sponge implantation model, in which a polyurethane sponge disk implanted subcutaneously in rats induces extensive angiogenesis in surrounding proliferative granuloma tissue (7, 8). With the use of this model, we have previously shown that angiogenesis both occurs concomitantly with the induction of COX-2 mRNA and is inhibited by administration either of a nonselective NSAID (indomethacin) or of selective COX-2 inhibitors (9). We further showed that PGE₂ or the PGI₂ analogue beraprost topically injected into the sponge promoted angiogenesis (9). Angiogenesis induced by either endogenous COX-2 or exogenous PGs was accompanied by increased expression of vascular endothelial growth factor (VEGF), and angiogenesis was abolished by administration of an antisense oligonucleotide specific for VEGF mRNA. These results suggest that either PGE₂ or PGI₂ may mediate the angiogenic action of COX-2 *in situ*.

PGs exert their biological actions by binding to specific receptors that contain seven transmembrane domains. Eight different PG receptors have been defined pharmacologically and cloned, including the PGD receptor (DP), four subtypes of PGE receptor (EP1, EP2, EP3, EP4), the PGF receptor (FP), the PGI receptor (IP), and the thromboxane (TX) receptor (TP) (10). Genes for each of these receptors have been disrupted and the corresponding knockout mice have been produced (11–16). Furthermore, with the use of the cloned receptors, agonists and antagonists highly selective for each of the four EP subtypes have been or are in the process of being developed (17–19).

With the use of these selective compounds and receptor knockout mice, we have now identified the PG species responsible for inducing angiogenesis in the sponge implantation model. Furthermore, we have characterized the role of PG signaling in tumor-associated angiogenesis and tumor progression in a mouse tumor implantation model. Our results indicate that host stromal PGE₂-EP3 signaling appears critical for tumor-associated angiogenesis and tumor growth, and that EP3 signaling pathway is relevant to the induction of a potent proangiogenic growth factor, VEGF, which certainly has a proangiogenic action. A highly selec-

tive EP3 antagonist therefore exhibits chemopreventive action on the stromal cells, and may become a novel therapeutic tool for cancer.

Materials and Methods

Tumor Implantation. Sarcoma 180 cells, which were originally isolated from CFW mice, were cultured at 37°C in RPMI 1640 medium supplemented with 10% fetal bovine serum under a humidified atmosphere containing 5% CO₂. The cells were suspended in phosphate-buffered saline at a density of 5 × 10⁷ cells/ml, and 100 μl of the resulting suspension were injected into the subcutaneous tissue of male mice. Lewis Lung carcinoma cells, which were originally isolated from C57BL/6 mice, were also used in the same manner with sarcoma 180 cells in some experiments (see Fig. 3 F). One half of each specimen was assayed for hemoglobin (Hb) content, whereas the other half was embedded in paraffin, sectioned (5 μm thickness), and stained with factor VIII antibody. Microvessel density was determined following our previous report (20). All animals were housed at a constant temperature (25 ± 1°C) and humidity (60 ± 5%). All experiments were performed in accordance with the guidelines for animal experiments of Kitasato University School of Medicine.

Sponge Implantation Model of Angiogenesis. Sponge disks (thickness, 5 mm; diameter, 1.3 cm; references 7 and 8) were implanted under light ether anesthesia into the subcutaneous tissues of the back of 8-wk-old male *ddy* mice, male EP3^{-/-} mice (14) and their wild-type counterparts, as well as IP^{-/-} mice (11) and the corresponding WT animals. Neovascularization was assessed by the same method as described above.

Prostaglandin Levels. Fluid within the sponge matrix enclosed by granulation tissue was gently aspirated with the use of a syringe equipped with a 25-gauge needle. The fluid was applied to a Sep-Pak C18 column, and PGs were then eluted with ethyl acetate. The eluate was dried, and the residue containing PGE₂ and 6-keto-PGF_{1α} were assayed with the use of specific ELISA (Cayman Chemical), as reported previously (21).

Immunohistochemistry. Tissue was immediately fixed with 4% paraformaldehyde in 0.1 M sodium phosphate buffer (pH 7.4), dehydrated with a graded series of ethanol solutions, and embedded in paraffin. Sections (4 μm in thickness) were prepared from the paraffin-embedded tissue and mounted on glass slides; after removal of paraffin with xylene, the slides were then placed in cold (4°C) acetone. The sections were subjected to either hematoxylin-eosin staining or immunostaining. For immunostaining, the sections were first exposed to diluted normal horse serum and then incubated with either rabbit antiserum to mouse COX-2 (Cayman Chemical), rabbit antiserum to mouse VEGF (Santa Cruz Biotechnology, Inc.), rabbit antiserum to mouse Mac-1 (BD Biosciences), or rabbit antiserum to mouse CD3e (BD Biosciences). Immune complexes were detected with a Vectastain ABC kit (Vector Laboratories).

In Situ Hybridization. For *in situ* hybridization, dissected tissue was sectioned with a cryostat, and the resulting sections were fixed with 4% paraformaldehyde. Digoxigenin-labeled antisense and sense riboprobes for mouse EP3 mRNA were prepared by *in vitro* transcription of the pCRII-TOPO vector (Invitrogen) containing mouse EP3. Sections were treated with proteinase K (10 μg/ml) and were then subjected to hybridization with labeled riboprobes in hybridization solution (Novagen) for 18 h at 50°C in moistened plastic boxes. They were then exposed to RNase A (20 μg/ml) and washed extensively, and hybridized probe was detected by *in*-

cubation first with alkaline phosphatase-conjugated antibodies to digoxigenin and then with 5-bromo-4-chloro-3 indolyl-phosphate and 4-nitroblue tetrazolium chloride (Roche Diagnostics). The specimens were finally counterstained with hematoxylin.

RT-PCR. Transcripts encoding EP1, EP2, EP3, EP4, VEGF, CD31, and glyceraldehyde-3-phosphate dehydrogenase (GAPDH) were quantified by RT-PCR analysis. Tissue was removed and rapidly frozen in liquid nitrogen. The frozen tissue was pulverized in a stainless steel cylinder cooled with liquid nitrogen. Total RNA was extracted from the tissue with ISOGEN (Wako), and cDNA was synthesized from 1 μ g of total RNA with the use of an oligo-p(dT)15 primer and AMV reverse transcriptase (Boehringer). 50 ng of cDNA were amplified with 1 U of Taq DNA polymerase in a 25 μ l reaction mixture containing 10 mM Tris-HCl (pH 8.3), 50 mM KCl, 1.5 mM MgCl₂, 0.2 mM of each deoxynucleoside triphosphate, and 0.6 μ M each of forward and reverse primers. The amplification protocol comprised 25 cycles (EP3, VEGF, CD31), 30 cycles (EP1), 40 cycles (EP2, EP4), or 20 cycles (GAPDH) of 45 s at 94°C, 60 s at 55°C, and 60 s at 72°C. The reaction mixtures were subsequently applied to a 2% agarose gel and the amplified products were stained with ethidium bromide. Primers used were as follows: 5'-AAT ACA TCT GTG GTG CTG CCA ACA-3' (sense) and 5'-CCA CCA TTT CCA CAT CGT GTG CGT-3' (antisense) for EP1, 5'-AGG ACT TCG CAG CCC CTT ACA CTT CTC CAA TG-3' (sense) and 5'-CAG CCC CTT ACA CTT CTC CAA ATG-3' (antisense) for EP2, 5'-GGAGAGACTCAGTGCA-GAAATATC-3' (sense) and 5'-GAACTGTTAGTGACACTGGGAATG-3' (antisense) for EP3, 5'-TTC CGC TCG TGG TGC GAG TGT TTC-3' (sense) and 5'-GAG GTG GTG TCT GCT TGG GTC AG-3' for EP4, 5'-AACCAT-GAACTTTCTGCTCTC-3' (sense) and 5'-GTGATTTTC-TGGCTTTGTTTC-3' (antisense) for VEGF, 5'-CGGGATC-CAGGAAAGCCAAGGCCAAA-3' (sense) and 5'-CGGAAT-TCTTGACTGTCTTAAGTTCC-3' (antisense) for CD31, and 5'-CCCTTCATTGACCTCAACTACAATGGT-3' (sense) and 5'-GAGGGGCCATCCACAGTCTTCTG-3' (antisense) for GAPDH.

Real Time RT-PCR. Isolation of RNA and reverse transcription was performed as described above. Before transcription, all RNA samples were treated with 1 μ g of DNase I (Life Technologies) per 1 μ g RNA. In addition, 2.5 μ g RNA from each sample was not reverse transcribed to ensure the effectiveness of the DNase treatment. Aliquots of 12.5 μ g of the cDNA and gene-specific primers were added to 25 μ l of qPCR Mastermix for Syber Green I (Eurogentec). Amplification reaction was performed and analyzed on ABI Prism 7700 Sequence Detector (Applied Biosystems). Primers for murine desmin were 5'-TCC CCG CTG AGC TCT CCC GTG TT-3' (sense) and 5'-AGC TCG CGC ATC TCC TCC TCG TAG-3' (antisense). Above mentioned primers for CD31 were also used. mRNA levels were normalized to β -actin mRNA and are presented as a ratio of desmin mRNA expression to CD31 mRNA.

Northern Blot Analysis. Total RNA (20 μ g) extracted from tissue as described above was fractionated by electrophoresis on a 1% agarose gel containing 2.2 M formaldehyde. The separated RNA molecules were transferred and covalently bound by alkaline fixation and ultraviolet radiation-induced cross-linking to a Hybond-N+ membrane (Amersham Biosciences). For preparation of mouse VEGF and GAPDH cRNA probes, 427- and 470-bp fragments of the respective cDNAs were cloned from RAW246.7 cells and sub-

cloned into the pGEM-T Easy vector (Promega). Plasmid DNA containing these fragments was linearized with NcoI or Sall, respectively, and then used as a template for synthesis of cRNA probes labeled with digoxigenin-UTP (Roche Diagnostics) by in vitro transcription with SP6 or T7 RNA polymerase. The presence of cRNA probes hybridized with mRNA on the membrane was detected with the use of alkaline phosphatase-conjugated antibodies to digoxigenin and the substrate CDP-Star (Roche Diagnostics). The membrane was exposed to x-ray film for visualization of chemiluminescence signals.

Gel Shift Assay. Primary cultured stromal fibroblasts of EP3 WT and EP3-knock out mice were stimulated with or without ONO-AE-248 (300 nM) in DMEM containing 10% FCS for 1 h. Double-stranded oligonucleotides containing consensus sequences were labeled with digoxigenin-11-ddUTP (Roche Diagnostics). The sense sequence of synthesized oligonucleotides used was 5'-CGC TTG ATG AGT CAG CCG GAA-3'. 20 μ g of the nuclear extracts of fibroblasts (passage 3) were incubated with 0.155 pmol of DIG-labeled AP-1 oligonucleotide in binding buffer (10 mM HEPES, 50 mM KCl, 5 mM MgCl₂, 0.5 mM EDTA, 5 mM DTT, 0.7 mM PMSF, 1 mg/ml poly(dI-dC)poly(dI-dC), pH 7.9) for 15 min at 25°C. For competition assay, 100-fold excess of unlabeled oligonucleotide was added to the binding reaction to the addition of the DIG-labeled probe. Then these incubation mixtures added electrophoresed in 6% native polyacrylamide gels with Tris borate-EDTA buffer. Detection of chemiluminescence was performed by using Gel Shift kit (Roche Diagnostics).

Drugs. Aspirin was provided by Merck, NS-398 (22) was obtained from Cayman Chemical, SC-560 (23) was provided by Searle (Skokie, IL), and JTE-522 (24) was kindly supplied by Japan Tobacco (Tokyo, Japan). EP receptor selective agonists, ONO-DI-004, ONO-AEI-257, ONO-AE-248, and ONO-AEI-329, which were developed by us previously (18), were topically injected to the sponges. An orally active, low molecular weight inhibitor of VEGF receptor (KDR/VEGFR 2) tyrosine kinase (ZD6474) (25) was a gift from AstraZeneca (Cheshire, UK).

We newly developed an EP3 antagonist, ONO-AE3-240. The Ki values of this antagonist obtained by competition-binding isotherms to displace the radioligand binding to the respective prostanoicid receptor are 590, 0.23, 58, and 1,500 nM for EP1, EP3, EP4, and FP, respectively, and more than 10 nM for EP2, DP, TP, and IP. Analysis of the agonistic and antagonistic actions showed that this compound acts as a selective antagonist at EP3 receptors. This inhibited the PGE₂ (10 nM)-induced increase in cytosolic Ca²⁺ concentration with median inhibitory concentrations of 1.5 nM for mouse EP3 receptor. This compound was dissolved in absolute ethanol at concentrations of 50 mM and 15 mM, and this stock solutions were diluted 100 times with physiological saline immediately before the topical injections. 3 d after the implantation of S-180 cells, the diluted solutions (0.1 ml/site) were subcutaneously injected around the tumors for 11 d twice a day. Physiological saline containing 1% ethanol was injected as vehicle control. An EP1 antagonist (ONO-8711; reference 17), and an EP4 antagonist (ONO-AE3-208; reference 19) were also topically injected around the tumors (twice a day, 50 nmole per tumor), in the same manner as ONO-AE3-240.

Statistical Analysis. Data are expressed as means \pm SEM. Comparisons among multiple groups were performed by factorial analysis of variance (ANOVA) followed by Scheffe's test. Comparisons between two groups were performed with Student's *t* test. A P value of <0.05 was considered statistically significant.

Results

The effects of COX inhibitors on tumor growth and angiogenesis were first tested using sarcoma 180 cells, which are allogeneic for ddy mice (Fig. 1). In control ddy mice treated with vehicle, solid tumors were apparent 14 d after cell implantation. Daily oral administration of SC-560, the inhibitor selectively acting on COX-1, had no significant effect on tumor mass. In contrast, the COX-2-selective inhibitors JTE-522 and NS-398 significantly reduced tumor mass, as did aspirin, a nonselective COX inhibitor (Fig. 1, A and D). The extent of tumor-induced angiogenesis was assessed on the basis of hemoglobin contents (Fig. 1 C), which correlated well with the vascular density in the tumor under histological examination (Fig. 1 B). Consistent with the marked red color of the tumors, angiogenesis was substantial in vehicle-treated mice (Fig. 1, B and C). Similar to the findings in tumor mass, angiogenesis was greatly reduced by treatment with COX-2 inhibitors or aspirin, but not with SC-560 (Fig. 1, B and C). These results suggested that COX-2 was involved in tumor growth and angiogenesis also in this model.

To test whether PGs generated by COX-2 are involved in angiogenesis and, if so, to identify a PG species and a PG receptor involved, we next employed a sponge implantation model that we developed previously. This model utilizes a polyurethane sponge implanted subcutaneously in mice, which induces proliferative granulation tissue around the implant and extensive angiogenesis within this encapsulation in a COX-2-dependent manner, thus mimicking the stromal angiogenic response around tumors. In the present experiment, to identify the receptor mediating the above action, we topically injected recently developed EP agonists that are highly selective for each subtypes. Neither the EP1 agonist ONO-DI-004, nor the EP2 agonist ONO-AEI-257, nor the EP4 agonist ONO-AEI-329 enhanced significant angiogenesis (Fig. 2 A). In contrast, the EP3 agonist ONO-AE-248 markedly increased the extent of angiogenesis in a dose-dependent manner (Fig. 2 A). Administration of ONO-AE-248 significantly increased the rate of angiogenesis, with the maximal effect at day 14 (Fig. 2 C). These were also true in the mice treated with a COX-2 selective inhibitor, JTE-522 (Fig. 2 B). These results suggest a role of the PGE₂-EP3 receptor signaling in the sponge-induced angiogenesis.

To verify the role of endogenous PGE₂, we applied the sponge model to mice deficient in EP3 receptor (EP3^{-/-}). We also used mice deficient in IP receptor (IP^{-/-}), because endogenous PGI₂ levels were increased in sponge implantation models. Their respective WT counterparts, were used as controls. The extent of angiogenesis in EP3^{-/-} mice was significantly reduced compared with that in WT mice (Fig. 2 D). In contrast, angiogenesis was significantly enhanced in IP^{-/-} mice compared with that in WT animals (unpublished data). The impaired angiogenic response in EP3^{-/-} mice was due to loss of receptors and not due to a difference in the production of PGs, as the amounts of PGE₂ and 6-keto-PGF_{1 α} , a stable metabolite of PGI₂, in the sponge implants

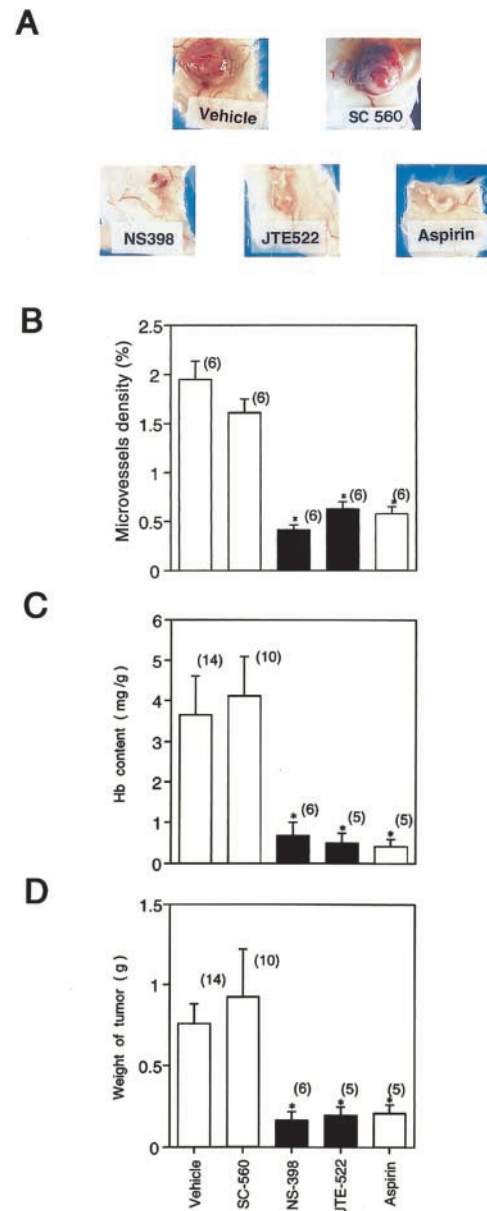


Figure 1. Effects of COX inhibitors on tumor growth and angiogenesis. (A) Typical appearance of tumors. A suspension of sarcoma 180 cells, which are allogeneic for ddy mice, was injected into subcutaneous tissue of ddy mice. COX inhibitors (SC-560, NS-398, and JTE-522, 3 mg/ml; aspirin, 10 mg/ml) were administered orally as a suspension (0.1 ml per 10 g of body mass) twice a day (every 12 h) beginning on the day of cell implantation and continuing throughout the 14-d experimental period. Tumors were then dissected and photographed. (B and C) The density of microvessels and hemoglobin content of tumor tissue were determined at the end of the 14-d experimental period. Data are means \pm SEM for the indicated number of tumors. * $P < 0.05$ versus vehicle-treated mice (ANOVA). (D) The mass of tumor tissue was determined at the end of the 14-d experimental period. All experiments were performed using male ddy mice. Data are means \pm SEM for the indicated number of tumors. * $P < 0.05$ versus vehicle-treated mice (ANOVA).

in EP3^{-/-} mice (345 ± 67 and 299 ± 28 pg per sponge, $n = 6$, respectively) were not significantly different from those in WT mice (260 ± 46 and 255 ± 39 pg per sponge, $n = 6$, respectively). The expressions of VEGF in sponge granula-

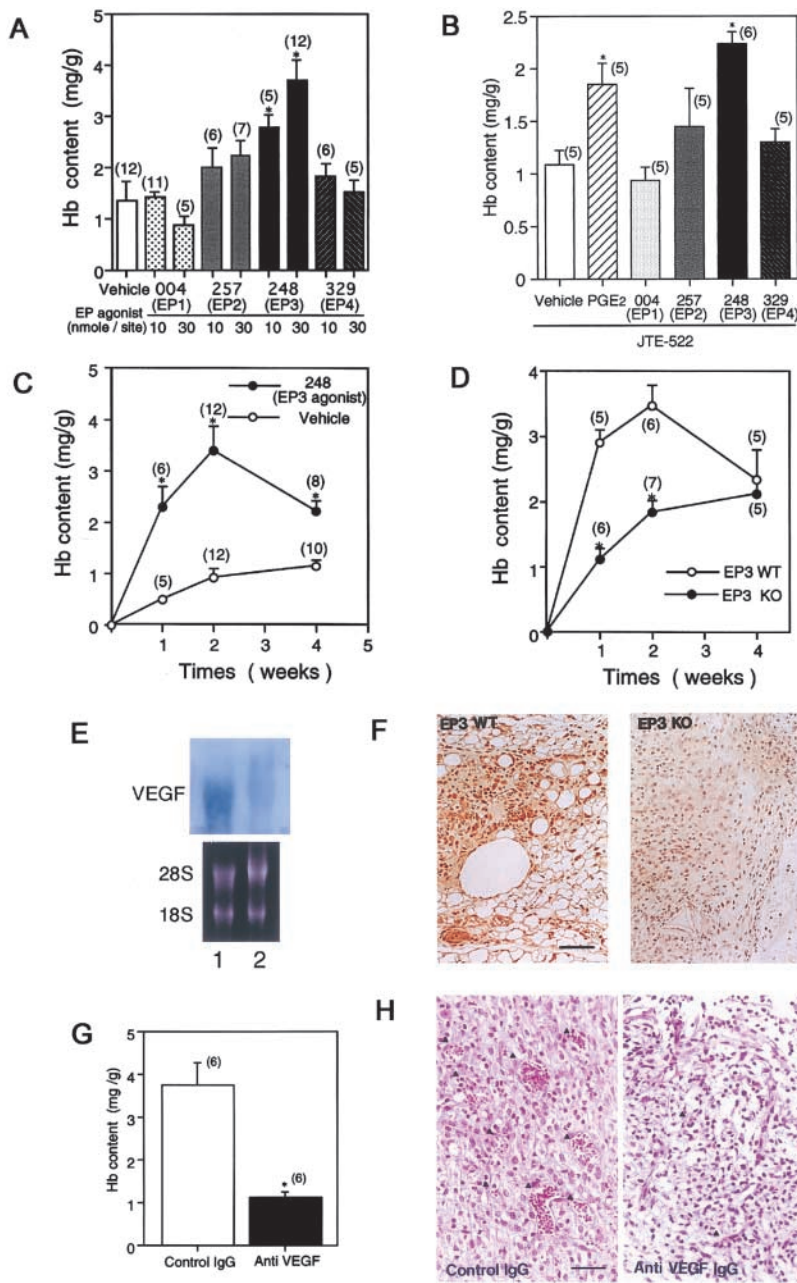


Figure 2. Angiogenesis in sponge-induced granulation tissues. (A) Hemoglobin content for male ddy mice treated with agonists selective for each EP subtype. ONO-DI-004 (EP1 agonist), ONO-AEI-257 (EP2 agonist), ONO-AE-248 (EP3 agonist), or ONO-AEI-329 (EP4 agonist) was topically injected into the implanted sponge over a period of 14 d (10 or 30 nmol per sponge per day) beginning on the day of implantation. Sponge-induced granulation tissue was dissected and its hemoglobin content was determined. Data are means \pm SEM for the indicated number of sponges (shown in parentheses). * $P < 0.05$ versus vehicle-injected sponges (ANOVA). (B) Hemoglobin content for COX-2 inhibitor-treated ddy mice receiving topical injections of EP subtype agonist. Each agonist was topically injected into the sponge over a period of 14 d (30 nmol per sponge per day). Sponge-induced granulation tissue was dissected and its hemoglobin content was determined. Data are means \pm SEM for the indicated number of sponges (shown in parentheses). * $P < 0.05$ versus vehicle-injected sponges (ANOVA). (C) Time courses of hemoglobin content during topical injections of an EP3 agonist, ONO-AE-248 (30 nmol per sponge per day). Data are means \pm SEM for the indicated number of sponges implanted in subcutaneous tissues. * $P < 0.05$ versus corresponding value for vehicle-injected sponges (ANOVA). (D) Time courses of sponge angiogenesis in EP3^{+/+} (WT) and EP3^{-/-} (KO) mice. Data are means \pm SEM for the indicated number of sponges. * $P < 0.05$ versus corresponding value for WT mice (ANOVA). (E) Northern blot analysis of VEGF mRNA. Sponge granulation tissue was isolated 14 d after the implantation in EP3^{+/+} mice (lanes 1) and EP3^{-/-} mice (lanes 2). Total RNA was prepared and subjected to Northern blot analysis of VEGF mRNA (top panel). The bottom panel also shows ethidium bromide staining of 28S and 18S mRNA. (F) Immunohistochemical localization of VEGF in sponge-induced granulation tissues. Sections of granulation tissue isolated from EP3^{+/+} (EP3 WT) and EP3^{-/-} (EP3 KO) mice 14 d after sponge implantation were stained with antibodies to VEGF. Scale bar, 50 μ m. (G) Effects of topical injections with antibodies to VEGF on angiogenesis. Sponges were implanted to in C57BL/6 WT mice treated with the EP3 agonist (30 nmol per site per day) for 14 d. Sponges were also injected with either IgG specific for mouse VEGF (10 μ g per sponge per day) or nonimmune control IgG. Data are means \pm SEM for the indicated number of sponges. * $P < 0.05$ versus sponges injected with control IgG (Student's *t* test). (H) Effects of topical injections with antibodies to VEGF on angiogenesis. Hematoxylin-eosin staining of sections prepared from granulation tissues in C57BL/6 WT mice. The arrows indicate neovascularized vessels. Scale bar, 50 μ m. The experiments were performed in male ddy mice (A–C), male EP3^{-/-} and WT C57BL/6 mice (D–F), and male WT C57BL/6 mice (G and H).

tion tissues were markedly reduced in EP3^{-/-} mice, compared with those in WT mice (Fig. 2, E and F). These results taken together demonstrate a significant role of endogenous PGE₂ in the sponge-induced angiogenesis, and suggest that EP3 receptor mediates this proangiogenic action of PGs. EP3 signaling is a major pathway for this angiogenesis, as topical injections of either EP3 agonist or PGE₂ did not enhance angiogenesis at all in EP3^{-/-} mice (data not shown). Expressed VEGF certainly enhanced angiogenesis in this model, as VEGF antibody significantly reduced angiogenesis compared with control IgG (Fig. 2, G and H).

We then investigated whether the PGE₂-EP3 signaling also operates in tumor-induced angiogenesis by comparing tumor growth and angiogenesis in four kinds of EP receptor knockout mice, IP^{-/-}, and their WT counterparts injected with sarcoma 180 cells. Sarcoma 180 cells are allogeneic for the prostanoid receptor knockout mice, which was developed from C57BL/6 mice. Solid tumors that formed in EP3^{-/-} mice were significantly smaller than those in WT mice (Fig. 3, B and D). Indeed, 14 d after the implantation of tumor cells, both tumor mass and angiogenesis, the latter assessed from microvessel density and hemoglobin

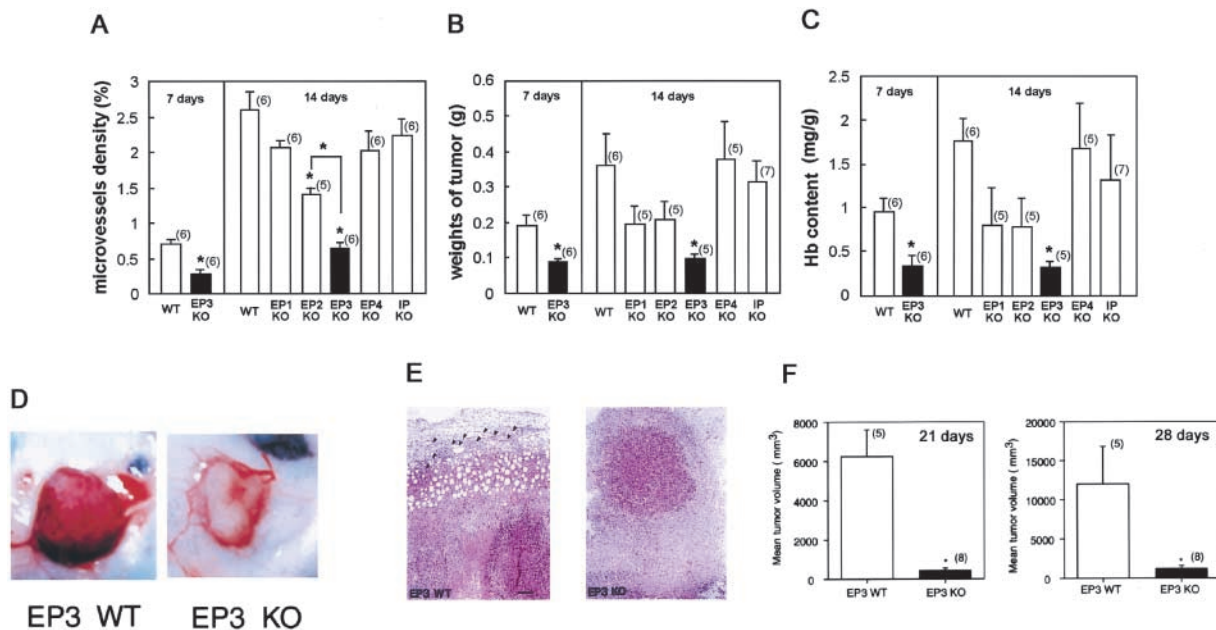


Figure 3. Tumor growth and angiogenesis in prostanoïd receptor knockout mice. Sarcoma 180 cells, which are allogeneic for C57BL/6 mice, were injected to the subcutaneous tissue of the back except the experiment shown in panel F. (A and C) Tumor-associated angiogenesis was determined by the density of microvessels and hemoglobin content 7 and 14 d after injection of sarcoma 180 cells. (B) Tumor weight was also measured. Data are means \pm SEM for the indicated number of tumors. * $P < 0.05$ versus corresponding value for WT mice (ANOVA). * $P < 0.05$, EP3 KO versus EP2 KO (Dunnett comparison). (D) Appearance of tumors. Tumors formed 14 d after injection of sarcoma 180 cells into (WT) and EP3^{-/-} (KO) mice were dissected and photographed. (E) Hematoxylin-eosin staining of tumors from (WT) and EP3^{-/-} (KO) mice. Scale bar, 100 μ m. (F) Tumor mass assessed 21 and 28 d after injection of another tumor cell line, Lewis Lung carcinoma cells suspension (5×10^7 cells/ml, 100 μ l/site) into the subcutaneous tissue of male mice. This cell line was syngeneic for C57BL/6 mice. The tumor volume was determined, as described before (reference 6). Data are means \pm SEM for the indicated number of tumors. * $P < 0.05$ versus WT animals (Student's *t* test). All experiments were performed using male C57BL/6 mice with and without disruption of EP receptor subtypes or IP receptor.

content, were significantly reduced in EP3^{-/-} mice compared with those in WT mice (Fig. 3 A–C). The extent of reduction in angiogenesis in EP3^{-/-} (by 76%) was certainly larger than that observed in EP2^{-/-} (by 46%), although angiogenesis in EP2^{-/-} mice was also significantly reduced when assessed by microvessel density (Fig. 3 A). Even in the early stage of the experiment (7 d after implantation), the reduced angiogenesis and tumor growth were observed (Fig. 3, A–C). Fig. 3 D shows typical appearance of tumors formed in EP3^{-/-} and WT mice. Histological examination of tumors formed in WT mice revealed an extensive vasculature in the capsule where tumors mingled with the surrounding normal tissue. In contrast, the tumors formed in EP3^{-/-} mice exhibited both a low level of vascularization and distinct boundaries with the surrounding normal tissue (Fig. 3 E). We observed a difference of tumor growth between EP3^{-/-} mice and WT mice using another neoplastic cell line, Lewis Lung carcinoma, which are syngeneic for C57BL/6 mice (Fig. 3 F). These results suggest that the EP3 receptor in the host has a major and critical role in tumor-induced angiogenesis and tumor growth. As shown below (see Fig. 5 A), the major EP receptor expressed in subcutaneous tissues in WT mice was EP3.

To corroborate the interaction between tumors (sarcoma 180) and the surrounding stroma, we examined COX-2 and VEGF expression in tumor and stromal tissue by immunohistochemical analysis in allogeneic models. Intense

staining for COX-2 was apparent in sarcoma cells of tumors that formed in WT mice; less marked staining was also apparent in the stromal cells surrounding the tumors in these animals (Fig. 4 A, left). Substantial COX-2 immunoreactivity was also detected in the tumors together with stromal cells that formed in EP3^{-/-} mice, although the extent of neovascularization in the capsular stroma was markedly reduced (Fig. 4 A, right). In WT mice, VEGF was abundant in surrounding stromal cells (Fig. 4 B, left), which major components were Mac-1 and CD3 double-negative fibroblast-like cells (Fig. 4, F and G), and was also present in smaller amounts in tumor cells (Fig. 4 B, left). The number of stromal cells, as well as of tumor cells, expressing VEGF was markedly reduced in EP3^{-/-} mice (Fig. 4 B, right). In situ hybridization revealed that EP3 mRNA was localized in both sarcoma and stromal cells (Fig. 4 C), but not in endothelial cells (Fig. 4 D, arrowhead), in WT mice, but was apparent only in the sarcoma cells in EP3^{-/-} mice (unpublished data).

RT-PCR analysis confirmed these findings on expression of VEGF and EP3 mRNA in tumor (sarcoma 180) and capsular stromal tissue (T+St) from WT mice and EP3^{-/-} mice. The expressed levels of other PGE receptor subtypes, EP1, EP2, and EP4, in both T+St and control subcutaneous tissue (H) were not apparently different between EP3^{-/-} mice and WT mice (Fig. 5 A). It further detected transcripts encoding CD31 in the tissue from WT mice but not

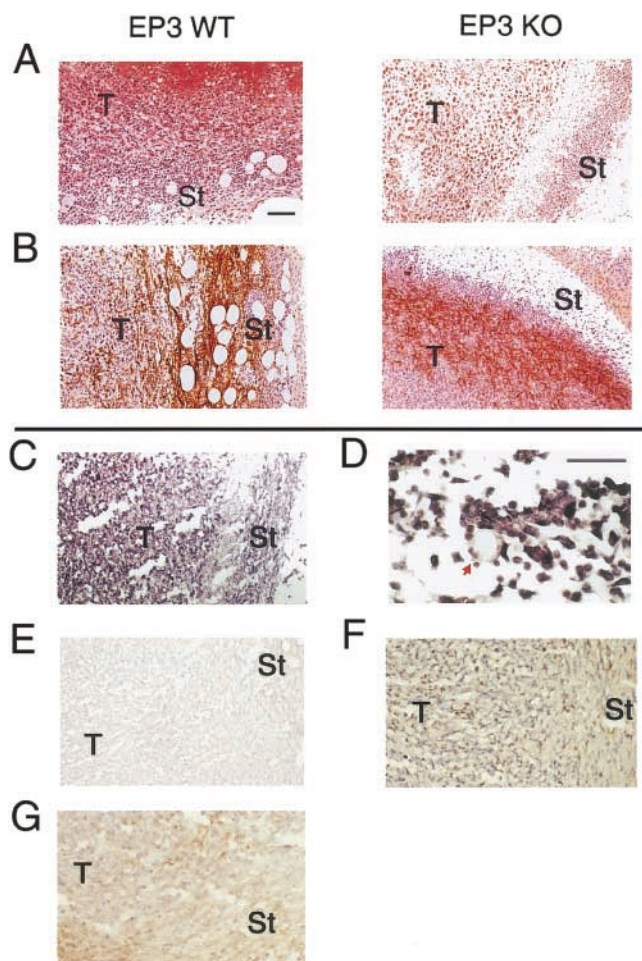


Figure 4. Expression of COX-2, VEGF, EP3 receptor in tumors and surrounding stroma tissues in WT mice and EP3 knockout mice 14 d after implantation of sarcoma 180 cells. (A) Immunohistochemical analysis of COX-2 expression in tumor (T) and stromal (St) tissue in WT EP3^{+/+} (EP3 WT, left) and EP3^{-/-} (EP3 KO, right) mice. COX-2 was apparent in both tumor cells and surrounding stromal cells, with no marked differences in the number of positive cells apparent between EP3^{-/-} mice and their WT counterparts. Scale bar, 100 μ m. (B) Immunohistochemical analysis of VEGF expression in tumor and stromal tissue in WT (left) and EP3^{-/-} (right) mice. VEGF-positive cells were apparent in the marginal zone of the tumor and in the surrounding stromal cells. Staining was more intense in wild-type mice than in EP3^{-/-} mice. (C–E) In situ hybridization analysis of EP3 mRNA in tumor and stromal tissue from WT mice. D, stromal tissue (high magnification, scale bar 10 μ m, arrowhead; neovascularization); E, results from control sense probe. (F) Immunohistochemical analysis of CD3e expression in tumor and stromal tissue in WT mice. (G) Immunohistochemical analysis of Mac-1 expression in tumor and stromal tissue in WT mice. All experiments were performed using male C57BL/6 mice with and without disruption of EP3 receptor. Sarcoma 180 cells, which are allogeneic for C57BL/6 mice, were injected to the subcutaneous tissues.

in that from EP3^{-/-} mice (Fig. 5 A). The ratio of the expression of desmin mRNA to that of CD31 mRNA determined in the samples isolated from the normal subcutaneous tissue (H) was not different between EP3^{-/-} mice and WT mice (Fig. 5 B). But, in the samples of sarcoma 180 tumors including surrounding stroma (T+ST), which were prepared in the same manner as PCR analysis experiment (Fig. 5 A), the ratio was reduced in both EP3^{-/-} mice and

WT mice, compared with that in the normal subcutaneous tissues isolated from each mouse (Fig. 5 B). Further, the reduction was more significant in EP3^{-/-} mice in comparison with that in WT mice (Fig. 5 B).

Daily topical injections of VEGF antibody significantly reduced tumor growth and angiogenesis in WT mice, but not in EP3^{-/-} mice, suggesting that VEGF is a predominant factor to induce tumor growth and angiogenesis in this model in response to EP3 signaling (Fig. 4 J). The lack of inhibition in tumor-associated angiogenesis in EP3^{-/-} mice was also observed in the mice treated with the inhibitor of tyrosine kinase of VEGF receptor, which was effective in WT mice (Fig. 5 E).

Gel shift assays of several transcriptional factors (AP-1, AP-2, SP-1, HIF-1, NF- κ B, and Oct-2A) in fibroblasts isolated from the stroma in EP3^{-/-} mice and WT mice, revealed that of the factors tested, AP-1 activation was significantly reduced in EP3^{-/-} mice, compared with WT mice, after stimulation with a selective agonist for EP3, ONO-AE-248 (Fig. 5 C). AP-1-dependent up-regulation of VEGF may be important in tumor-associated angiogenesis mediated by EP3 receptors.

Recently, we succeeded to develop a potent and selective EP3 antagonist, ONO-AE3-240. Daily topical injections of this EP3 antagonist around the tumor (sarcoma 180) significantly suppressed tumor-associated angiogenesis and tumor growth in WT mice, whereas those of an EP1 antagonist and an EP4 antagonist did not (Fig. 6 A). This chemopreventive effect of an EP3 antagonist was not seen in EP3^{-/-} mice (Fig. 6 B).

Discussion

Treatment with NSAIDs limits tumor growth and metastatic potential in various model systems as well as clinically in cancer patients (26–29). Of the two COX isozymes, COX-2 appears to play the predominant role in tumor growth (2, 28, 29), although the underlying mechanism has remained unclear. The antiapoptotic potential of PGE₂ has been suggested to contribute to colorectal carcinogenesis (30). With the use of a synthetic antagonist specific for EP1 together with mice deficient in this receptor, Watanabe et al. (17) showed that EP1 contributes to the formation of precancerous lesions induced by the colon carcinogen azoxymethane. However, the effects of the antagonist and of receptor disruption were limited to partial inhibition, leaving open the possibility that additional COX-2-dependent mechanisms are important in carcinogenesis.

An important factor in the promotion of tumor growth is angiogenesis (31, 32). Substantial increases in tumor mass must be preceded by an increase in blood supply to provide the nutrients and oxygen required for tumor growth. It has been suggested that the mechanisms for promotion of angiogenesis are activated in the early stages of tumor development (33). We have now shown with our sarcoma 180 implantation model that COX-2-selective inhibitors inhibited tumor growth and associated angiogenesis. The COX-2 blockers inhibited tumor growth by ~80%, similar

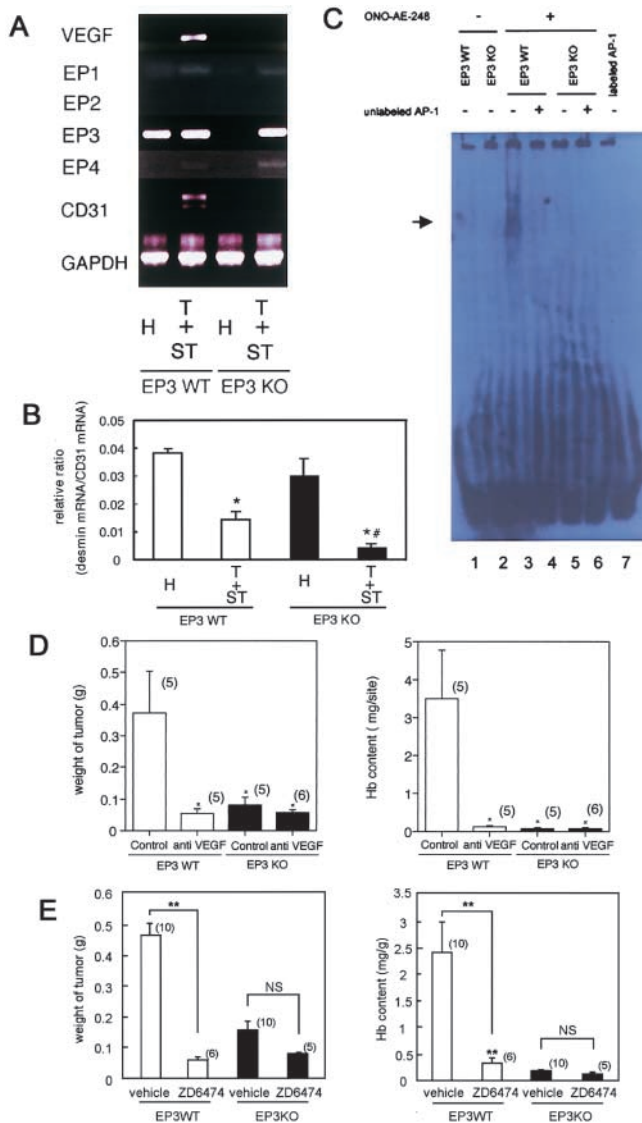


Figure 5. Expression of VEGF, EP receptor subtypes, and CD31 in tumors and surrounding stroma tissues in C57BL/6 WT mice and EP3 knockout mice, and effects of a VEGF neutralizing antibody and a VEGF receptor kinase inhibitor on tumor growth and tumor-associated angiogenesis. Sarcoma 180 cells, which are allogeneic for C57BL/6 mice, were injected to the subcutaneous tissues. (A) RT-PCR analysis of EP1, EP2, EP3, EP4, VEGF, and CD31 mRNAs in tumor tissue dissected together with surrounding stroma (T + St), as well as in control subcutaneous tissue (H) dissected from sites distant from tumors, of WT and EP3^{-/-} mice. 14 d after implantation, sample tissues were isolated. (B) A ratio of desmin mRNA/CD31 mRNA. Real time RT-PCR analysis was performed as described in the methods, and a ratio of the expression of desmin mRNA to that of CD31 mRNA was determined. Data are means \pm SEM for 4 samples prepared as above. * $P < 0.05$ compared with H, and # $P < 0.05$ compared with T+ST in EP3WT (ANOVA). (C) Gel shift assay. Primary cultured fibroblasts from WT and EP3^{-/-} mice were stimulated with ONO-AE-248, an EP3 agonist. Activation of AP-1 was determined by EMSA. Lanes 1, 2, and 7, or 3 to 6, without or with ONO-AE-248; lanes 4 and 6, presence of unlabeled oligonucleotide with nuclear extract, by which specificity was evaluated by oligonucleotide competition and EMSA; lane 7, control oligonucleotide without nuclear extract. (D and E) Effects of an anti-VEGF antibody and a VEGF receptor kinase inhibitor on tumor growth and angiogenesis in WT and EP3^{-/-} mice. Tumor-associated angiogenesis was determined 14 d after injection of sarcoma 180 cells. Either IgG specific for mouse

to the extent of the effect of such inhibitors on the growth of COX-2-overexpressing tumor cells transplanted into nude mice (6). These latter researchers also showed that the promotion of tube formation by human umbilical vein endothelial cells induced by cocultured Caco-2 cells that overexpress COX-2 is mediated through the production and release of proangiogenic factors by the tumor cells themselves. If such a mechanism also operates in vivo, tumor-associated angiogenesis would depend only on tumor cells. However, we have now shown that not only angiogenesis but also tumor growth were significantly reduced in EP3^{-/-} mice compared with those in WT mice, although the transplanted tumor cells expressed EP3 receptors. These results strongly suggested that the host stromal PGE₂-EP3 signaling was important in tumor-associated angiogenesis and tumor growth.

To mimic stromal angiogenic responses, we developed the sponge implantation model. Two advantages of this model for studies of angiogenesis are that angiogenesis can be readily quantified by measurement of the hemoglobin content of the sponge-induced granulation tissue together with histological examination, and that the effects of exogenous substances can be investigated by their direct injection into the sponge (7–9). The EP3 agonist ONO-AE-248 specifically enhanced angiogenesis in this model in a dose-dependent manner, and further the angiogenic response was certainly reduced in EP3^{-/-} with the reduction of VEGF expression, suggesting that endogenous PGE₂ facilitates angiogenesis through the EP3 signaling and the induction of VEGF in this model. Previous studies with various cell lines have indicated that PGE₂ induces VEGF expression through a cAMP-dependent mechanism (34, 35). We previously reported that PGE₂ induces VEGF through the activation of adenylate cyclase/protein kinase A signaling pathway (36). One of the EP3 splicing variants (37, 38), which may couple to the elevation in intracellular cAMP levels, may enhance angiogenesis in this model.

It has been previously reported that E type PGs have a proangiogenic activity in corneal test (39) and in the chorioallantoic membrane (CAM) technique (40). Further, Form and Auerbach reported that PGE₂ strongly induced angiogenesis on CAM of 8-d-old chicken embryos, but PGA₂, PGF_{2 α} , and a derivative of TXA₂ did not. A recent report (41) described that the endothelial migration was mediated by COX-2 and TXA₂, but this experiment was performed using confluent monolayer endothelial cells stimulated with PMA. The authors also reported that corneal angiogenesis was suppressed with COX-2 inhibitor and TXA₂ antagonist, the former of which inhibited more strongly than the latter, suggesting the involvement of

VEGF (10 μ g per tumor per day, once a day) or nonimmune control IgG was topically injected around the tumors (D). Either VEGF receptor kinase inhibitor, ZD6474 (100 mg/kg, once a day) or vehicle control solution was orally administered (E). Data are means \pm SEM for the indicated number of tumors. * $P < 0.05$ compared with WT mice receiving control IgG or vehicle solution (ANOVA).

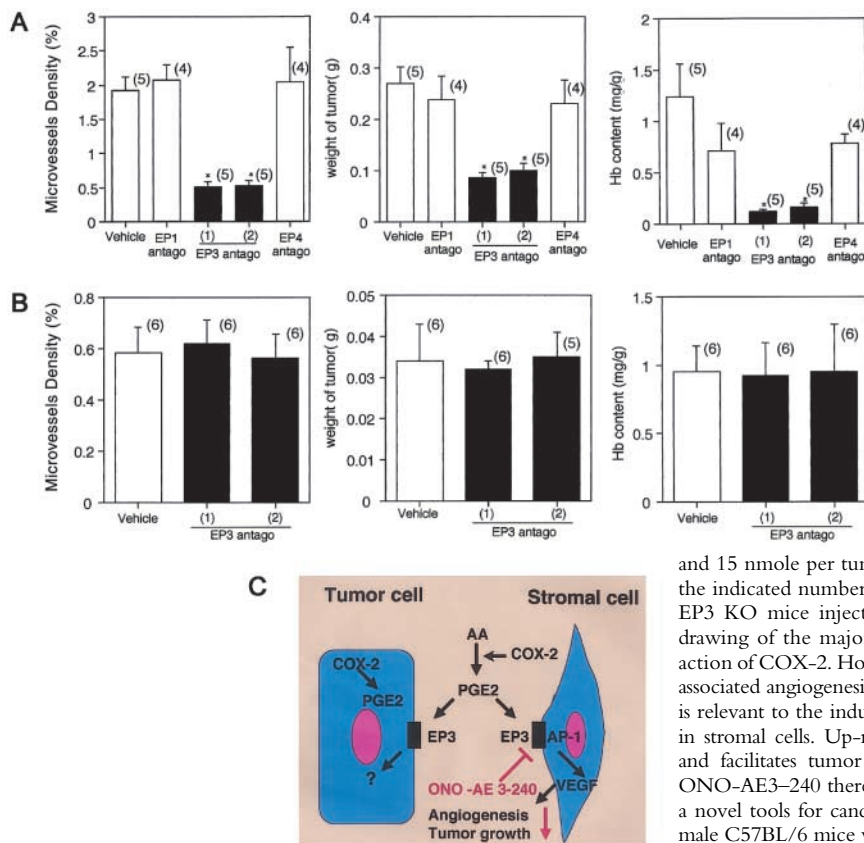


Figure 6. Effect of an EP3 antagonist on tumor growth and tumor-associated angiogenesis. Sarcoma 180 cells, which are allogeneic for C57BL/6 mice, were injected to the subcutaneous tissues. (A) Tumor-associated angiogenesis was determined in WT mice by the density of microvessels 14 d after the injection. Tumor weight was also determined 14 d after the injection. An EP1 antagonist (EP1 antago, ONO-8711), an EP3 antagonist (EP3 antago, ONO-AE3-240), or an EP4 antagonist (EP4 antago, ONO-AE3-208) was topically injected around the tumors (twice a day, 50 nmole per tumor). EP3 antago (1) and (2); twice a day, 50 and 15 nmole per tumor, respectively. Data are means \pm SEM for the indicated number of tumors. * $P < 0.05$ versus corresponding value for WT mice injected with vehicle solution (ANOVA). (B) Tumor growth and tumor-associated angiogenesis were determined in EP3^{-/-} (KO) mice 14 d after injection of sarcoma 180 cells. An EP3 antagonist (ONO-AE3-240) was topically injected around the tumors. EP3 antago (1) and (2); 50 and 15 nmole per tumor per day, respectively. Data are means \pm SEM for the indicated number of tumors. * $P < 0.05$ versus corresponding value for EP3 KO mice injected with vehicle solution (ANOVA). (C) Schematic drawing of the major signaling pathway of PGE₂ generated through the action of COX-2. Host stromal PGE₂-EP3 signaling appears critical for tumor-associated angiogenesis and tumor growth. EP3 signaling on the stromal cells is relevant to the induction of a potent proangiogenic growth factor, VEGF in stromal cells. Up-regulated VEGF certainly has a proangiogenic action, and facilitates tumor growth. A highly selective EP3 antagonist such as ONO-AE3-240 therefore exhibits chemopreventive action, and will become a novel tools for cancer prevention. All experiments were performed using male C57BL/6 mice with and without disruption of EP3 receptor.

other COX-2 products than TXA₂. However, these *in vivo* results were obtained under bFGF-stimulated conditions. In our separate experiment, angiogenesis in the sponge implantation model under no stimulation was not reduced with either a thromboxane synthase inhibitor, OKY046 or a TP receptor antagonist, S-1452 (unpublished data). The contribution of TP receptor signaling to tumor-associated angiogenesis should be estimated carefully. In the present experiments, we tested tumor-associated angiogenesis in knockout mice of EP subtypes or IP receptors (Fig. 3, A and C). As shown in the present study, not only tumor growth but also tumor-associated angiogenesis are highly dependent on EP3 receptor signaling. Judging from the time course of changes in size and angiogenesis of tumors in EP3^{-/-} and WT mice (Fig. 3, A–C), the reduced tumor growth and angiogenesis in EP3^{-/-} mice is not a simply minor delay. However, angiogenesis and growth of polyps in mice with a mutated APC gene were recently reported to be EP2-dependent (42, 43). Their report described that the major elements which express COX-2 are stromal cells around the tumors or intestinal polyps. We identified that the cells which produced VEGF to facilitate angiogenesis and tumor growth were CD3 and Mac-1 double-negative fibroblasts. It is widely known that the fibroblasts exhibit heterogeneity in term of various biological factors including prostaglandin generating systems and receptor systems (44–46). We have shown in the present study, not only tumor growth but also tumor-associated angiogenesis are highly EP3 dependent. They did not show

the microvessel density in EP3^{-/-} with APC mutation in their recent report (43), and the reduction percentage of angiogenesis in APC-mutated EP2^{-/-} mice was $\sim 30\%$ at best. As shown in Fig. 5 A, the major EP receptor expressed in subcutaneous tissues in WT mice was EP3, which did not expressed in the intestine (43). These suggested that tumor-associated angiogenesis may be regulated in a site-specific fashion, and may be related to the heterogeneity of the stromal fibroblasts.

The mouse strains, ddy mouse and C57BL/6 mouse are allogeneic for S-180 sarcoma cell line used in the present study. However, we tested another cell line, Lewis lung carcinoma, for which C57BL/6 mouse is syngeneic (Fig. 3 F). The difference of tumor growth in EP3^{-/-} mice and WT counterparts was observable in both tumor cell lines. These suggested that EP3 receptor signaling to facilitate the tumor growth was important not only in allogeneic tumors but also in syngeneic tumors.

The host microenvironment is thought to influence tumor progression (47, 48). Examination of human colorectal cancer tissue has revealed marked COX-2 expression not only in cancer cells but also in inflammatory cells and fibroblasts that surround the cancer cells (34). Ohshima et al. (2) also showed that COX-2 is abundant in the stromal cells that surround intestinal polyps in mice with a mutated APC gene. Recent results using COX-2 knockout mice also supported the significance of stromal COX-2 in tumor-induced angiogenesis and tumor growth (49). In the present study, we have focused on the down-stream signal-

ing pathway after COX-2 induction. We detected marked VEGF immunoreactivity in host stromal cells, including fibroblast-like cells, that surrounded the implanted sarcoma cells in EP3^{+/+} mice but not in the corresponding cells of EP3^{-/-} mice, suggesting that these stromal cells express VEGF in response to activation of EP3 receptors by endogenous PGE₂. We therefore propose that COX-2 expressing stromal cells around the tumors and/or tumor cells themselves synthesize and release PGE₂ into the tumor microenvironment, and that PGE₂ then acts on the stromal cells expressing EP3 receptors to induce the production of proangiogenic factors and consequent angiogenesis.

It is interesting to see whether or not EP3 receptor signaling enhances the stability of the newly formed vessels by modulating periendothelial cells which invest the vessels. Desmin was reported to be expressed in the pericytes on the tumor blood vessels, where the loose association of pericytes with endothelium (50). We performed real time PCR to determine a ratio of the expression of desmin mRNA to that of CD31 mRNA (Fig. 5 B). As the expression of CD31 is dependent on the proliferation of the endothelial cells on newly formed vessels, it is plausible that this ratio neatly correlates with the development of investment of pericytes on the blood vessels. The ratio determined in the samples isolated from the normal subcutaneous tissue (H) was not different between EP3^{-/-} mice and WT mice. But, in the samples of S-180 tumors including surrounding stroma (T+ST), the ratio was reduced in both EP3^{-/-} mice and WT mice, compared with that in the normal subcutaneous tissues isolated from each mouse. Further, the reduction was more significant in EP3^{-/-} mice in comparison with that in WT mice. These results taken together suggest that the development of pericytes on the newly formed vessels in association to tumors is EP3 receptor signaling-dependent, and that the equipment of the pericytes in the vessels (arterioles and venules) in normal tissues is not.

Among the various factors, VEGF may be a candidate to enhance angiogenesis in sponge model judging from the results using VEGF neutralizing antibody (Fig. 2, G and H). Further, daily topical injections of VEGF antibody significantly reduced tumor growth and angiogenesis in WT mice, but not in EP3^{-/-} mice (Fig. 5 D), suggesting that VEGF is a predominant factor to induce tumor growth and angiogenesis in host microenvironment. The results from VEGF receptor tyrosine kinase inhibitor concrete this finding (Fig. 5 E).

Gel shift assays of several transcriptional factors in stromal fibroblasts, revealed that AP-1 activation was significantly reduced in EP3^{-/-} mice, compared with EP3^{+/+} mice with an EP3 agonist (Fig. 5 I), suggesting that AP-1-dependent up-regulation of VEGF may be important in tumor-associated angiogenesis mediated by EP3 receptors. AP-1-dependent VEGF expression was also reported in several kinds of cells (51, 52).

To concrete the results so far obtained with EP3^{-/-} mice, we topically injected an EP3 receptor antagonist, which we recently developed. Daily topical injections of an EP3 antagonist to the subcutaneous tissues around the tumor, where functionally active EP3 receptors are localized,

significantly suppressed tumor-associated angiogenesis and tumor growth in WT mice, whereas those of an EP1 antagonist and an EP4 antagonist did not (Fig. 6 A). This chemopreventive effect of an EP3 antagonist was not seen in EP3^{-/-} mice (Fig. 6 B). These results certainly confirm the results from EP3^{-/-} mice.

In conclusion, as shown in Fig. 6 C, host stromal PGE₂-EP3 signaling appears critical for tumor-associated angiogenesis and tumor growth. EP3 signaling on the stromal cells was relevant to the induction of a potent proangiogenic growth factor, VEGF in stromal cells. Up-regulated VEGF certainly has a proangiogenic action, and facilitates tumor growth. A highly selective EP3 antagonist therefore exhibits chemopreventive action on the stromal cells, and will become a novel therapeutic tool for cancer. The results presented here neatly provide an answer to the question how NSAIDs prevent tumor development.

We thank Michiko Ogino, Keiko Nakamigawa, Osamu Katsumata, and Masaki Soma for technical assistance.

This work was supported by research grants (no. 12470529 and no. 12670094), by "High-tech Research Center" grant, and by Academic Frontier Project grant from the Ministry of Education, Culture, Sports, Science and Technology. This study was also supported by an Integrative Research Program of the Graduate School of Medical Science, Kitasato University, and by a grant from Terumo life science foundation.

Submitted: 13 August 2002

Revised: 2 December 2002

Accepted: 4 December 2002

References

- Smalley, W., and R.N. Dubois. 1997. Colorectal cancer and non steroidal anti-inflammatory drugs. *Adv. Pharmacol.* 39:1-20.
- Ohshima, M., J.E. Dinchuk, S.L. Kargman, H. Oshima, B. Hancock, E. Kwong, J.M. Trzaskos, J.F. Evans, and M.M. Taketo. 1996. Suppression of intestinal polyposis in *Apc*^{Δ716} knockout mice by inhibition of cyclooxygenase 2 (COX-2). *Cell.* 87:803-809.
- Marx, J. 2001. Cancer research. Anti-inflammatories inhibit cancer growth—but how? *Science.* 291:581-582.
- Prescott, S.M., and R.L. White. 1996. Self-promotion? Intimate connections between APC and prostaglandin H synthase-2. *Cell.* 87:783-786.
- Shiff, S.J., and B. Rigas. 1997. Nonsteroidal anti-inflammatory drugs and colorectal cancer: evolving concepts of their chemopreventive actions. *Gastroenterology.* 113:1992-1998.
- Tsuji, M., S. Kawano, S. Tsuji, H. Sawaoka, H. Hori, and R.N. DuBois. 1998. Cyclooxygenase regulates angiogenesis induced by colon cancer cells. *Cell.* 93:705-716.
- Majima, M., M. Isono, Y. Ikeda, I. Hayashi, K. Hatanaka, Y. Harada, O. Katsumata, S. Yamashina, M. Katori, and S. Yamamoto. 1997. Significant roles of inducible cyclooxygenase (COX)-2 in angiogenesis in rat sponge implants. *Jpn. J. Pharmacol.* 75:105-114.
- Muramatsu, M., J. Katada, I. Hayashi, and M. Majima. 2000. Chymase as a proangiogenic factor. A possible involvement of chymase-angiotensin-dependent pathway in the hamster sponge angiogenesis model. *J. Biol. Chem.* 275:5545-5552.

9. Majima, M., I. Hayashi, M. Muramatsu, J. Katada, S. Yamashina, and M. Katori. 2000. Cyclooxygenase-2 enhances basic fibroblast growth factor-induced angiogenesis through the induction of vascular endothelial growth factor in rat sponge implants. *Br. J. Pharmacol.* 130:641–649.
10. Narumiya, S., Y. Sugimoto, and F. Ushikubi. 1999. Prostanoid receptors: structures, properties, and function. *Physiol. Rev.* 79:1193–1226.
11. Murata, T., F. Ushikubi, T. Matsuoka, M. Hirata, A. Yamasaki, Y. Sugimoto, A. Ichikawa, Y. Aze, T. Tanaka, N. Yoshida, A. Ueno, S. Oh-ishi, and S. Narumiya. 1997. Altered pain perception and inflammatory responses in mice lacking prostacyclin receptor. *Nature.* 388:678–682.
12. Sugimoto, Y., A. Yamasaki, E. Segi, K. Tsuboi, Y. Aze, T. Nishimura, H. Oida, N. Yoshida, T. Tanaka, M. Katsuyama, et al. 1997. Failure of parturition in mice lacking the prostaglandin F receptor. *Science.* 277:681–683.
13. Segi, E., Y. Sugimoto, A. Yamasaki, Y. Aze, H. Oida, T. Nishimura, T. Murata, F. Ushukubi, M. Fukumoto, T. Tanaka, et al. 1998. Patent ductus arteriosus and neonatal death in prostaglandin receptor EP4-deficient mice. *Biochem. Biophys. Res. Commun.* 246:7–12.
14. Ushikubi, F., E. Segi, Y. Sugimoto, T. Murata, T. Matsuoka, T. Kobayashi, H. Hizaki, K. Tsuboi, M. Katsuyama, A. Ichikawa, et al. 1998. Impaired febrile response in mice lacking the prostaglandin E receptor subtype EP3. *Nature.* 395:281–284.
15. Hizaki, H., E. Segi, Y. Sugimoto, M. Hirose, T. Saji, F. Ushikubi, T. Matsuoka, Y. Noda, T. Tanaka, N. Yoshida, et al. 1999. Abortive expansion of the cumulus and impaired fertility in mice lacking the prostaglandin E receptor subtype EP2. *Proc. Natl. Acad. Sci. USA.* 96:10501–10506.
16. Matsuoka, T., M. Hirata, H. Tanaka, Y. Takahashi, T. Murata, K. Kabashima, Y. Sugimoto, T. Kobayashi, F. Ushikubi, Y. Aze, et al. 2000. Prostaglandin D₂ as a mediator of allergic asthma. *Science.* 287:2013–2017.
17. Watanabe, K., T. Kawamori, S. Nakatsugi, T. Ohta, S. Ohichida, H. Yamamoto, T. Matuyama, K. Kondo, F. Ushikubi, S. Narumiya, T. Sugimura, and K. Wakabayashi. 1999. Role of the prostaglandin E receptor subtype EP1 in colon carcinogenesis. *Cancer Res.* 59:5093–5096.
18. Suzawa, T., C. Miyaura, M. Inada, T. Maruyama, Y. Sugimoto, F. Ushikubi, A. Ichikawa, S. Narumiya, and T. Suda. 2000. The role of prostaglandin E receptor subtypes (EP1, EP2, EP3 and EP4) in bone resorption: an analysis using specific agonists for respective EPs. *Endocrinology.* 141:1554–1559.
19. Kabashima, K., T. Saji, T. Murata, M. Nagamachi, T. Matsuoka, E. Segi, K. Tsuboi, Y. Sugimoto, T. Kobayashi, Y. Miyachi, et al. 2002. The prostaglandin receptor EP4 suppresses colitis, mucosal damage and CD4 cell activation in the gut. *J. Clin. Invest.* 109:883–893.
20. Fujita, M., I. Hayashi, S. Yamashina, M. Itoman, and M. Majima. 2002. Blockade of angiotensin AT1a receptor signaling reduces tumor growth, angiogenesis, and metastasis. *Biochem. Biophys. Res. Commun.* 294:441–447.
21. Boku, K., T. Ohno, T. Saeki, H. Hayashi, I. Hayashi, M. Katori, T. Murata, S. Narumiya, K. Saigenji, and M. Majima. 2001. Adaptive cytoprotection mediated by prostaglandin I₂ is attributable to sensitization of CRGP-containing sensory nerves. *Gastroenterology.* 120:134–143.
22. Futaki, N., K. Yoshikawa, Y. Hamasaka, I. Arai, S. Higuchi, H. Iizuka, and S. Otomo. 1993. NS-398, a novel non-steroidal anti-inflammatory drug with potent analgesic and antipyretic effects, which causes minimal stomach lesions. *Gen. Pharmacol.* 24:105–110.
23. Smith, C.J., Y. Zhang, C.M. Koboldt, J. Muhammad, B.S. Zweifel, A. Shaffer, J.J. Talley, J.L. Masferrer, K. Seibert, and P.C. Isakson. 1998. Pharmacological analysis of cyclooxygenase-1 in inflammation. *Proc. Natl. Acad. Sci. USA.* 95:13313–13318.
24. Wakitani, K., T. Nanayama, M. Masaki, and M. Matsushita. 1998. Profile of JTE-522 as a human cyclooxygenase-2 inhibitor. *Jpn. J. Pharmacol.* 78:365–371.
25. Wedge, S.R., D.J. Ogilvie, M. Dukes, J. Kendrew, R. Chester, J.A. Jackson, S.J. Boffey, P.J. Valentine, J.O. Curwen, H.L. Musgrove, et al. 2002. ZD6474 inhibits vascular endothelial growth factor signaling, angiogenesis, and tumor growth following oral administration. *Cancer Res.* 62:4645–4655.
26. Tsujii, M., S. Kawano, and R.N. DuBois. 1997. Cyclooxygenase-2 expression in human colon cancer cells increases metastatic potential. *Proc. Natl. Acad. Sci. USA.* 94:3336–3340.
27. Masferrer, J.L., A. Koki, and K. Seibert. 1999. COX-2 inhibitors. A new class of antiangiogenic agents. *Ann. NY Acad. Sci.* 889:84–86.
28. Sawaoka, H., S. Tsuji, M. Tsujii, E.S. Gunawan, Y. Sasaki, S. Kawano, and M. Hori. 1999. Cyclooxygenase inhibitors suppress angiogenesis and reduce tumor growth in vivo. *Lab. Invest.* 79:1469–1477.
29. Williams, C.S., M. Mann, and R.N. DuBois. 1999. The role of cyclooxygenases in inflammation, cancer, and development. *Oncogene.* 18:7908–7916.
30. Tsujii, M., and R.N. DuBois. 1995. Alterations in cellular adhesion and apoptosis in epithelial cells overexpressing prostaglandin endoperoxide synthase-2. *Cell.* 83:493–501.
31. Folkman, J. 1971. Tumor angiogenesis: therapeutic implications. *N. Engl. J. Med.* 285:1182–1186.
32. Folkman, J. 1996. What is the evidence that tumors are angiogenesis dependent? *J. Natl. Cancer Inst.* 82:4–6.
33. Hanahan, D., and J. Folkman. 1996. Patterns and emerging mechanisms of angiogenic switch during tumorigenesis. *Cell.* 86:353–364.
34. Harada, S., J.A. Nagy, K.A. Sullivan, K.A. Thomas, N. Endo, G.A. Rodan, and S.B. Rodan. 1994. Induction of vascular endothelial growth factor expression by prostaglandin E₂ and E₁ in osteoblasts. *J. Clin. Invest.* 93:2490–2496.
35. Hoper, M.M., N.F. Voelkel, T.O. Bates, J.D. Allard, M. Horan, D. Shepherd, and R.M. Tuder. 1997. Prostaglandins induce vascular endothelial growth factor in a human monocytic cell line and rat lungs via cAMP. *Am. J. Respir. Cell Mol. Biol.* 17:748–756.
36. Amano, H., K. Ando, S. Minamida, I. Hayashi, M. Ogino, S. Yamashina, H. Yoshimura, and M. Majima. 2001. Adenylate cyclase/protein kinase A signaling pathway enhances angiogenesis through induction of vascular endothelial growth factor in vivo. *Jpn. J. Pharmacol.* 87:181–188.
37. Namba, T., Y. Sugimoto, M. Negishi, A. Irie, F. Ushikubi, A. Kakizuka, S. Ito, A. Ichikawa, and S. Narumiya. 1993. Alternative splicing of C-terminal tail of prostaglandin E receptor subtype EP3 determines G-protein specificity. *Nature.* 365:166–170.
38. Sugimoto, Y., M. Negishi, Y. Hayashi, T. Namba, A. Honda, A. Watabe, M. Hirata, S. Narumiya, and A. Ichikawa. 1993. Two isoforms of the EP3 receptor with dif-

- ferent carboxy-terminal domains. Identical ligand binding properties and different coupling properties with Gi proteins. *J. Biol. Chem.* 268:2712–2718.
39. Ziche, M., J. Jones, and P.M. Gullino. 1982. Role of prostaglandin E1 and copper in angiogenesis. *J. Natl. Cancer Inst.* 69:475–482.
 40. Spisni, E., F. Manica, and Y. Tomasi. 1992. Involvement of prostanoids in the regulation of angiogenesis by polypeptide growth factors. *Prostaglandins Leukot. Essent. Fatty Acids.* 47: 111–115.
 41. Daniel, T.O., H. Liu, J.D. Morrow, B.C. Crews, and L.J. Marnett. 1999. Thromboxane A2 is a mediator of cyclooxygenase-2-dependent endothelial migration and angiogenesis. *Cancer Res.* 59:4574–4577.
 42. Seno, H., M. Oshima, T.O. Ishikawa, H. Oshima, K. Takaku, T. Chiba, S. Narumiya, and M.M. Taketo. 2002. Cyclooxygenase 2- and prostaglandin E(2) receptor EP(2)-dependent angiogenesis in Apc(Delta716) mouse intestinal polyps. *Cancer Res.* 62:506–511.
 43. Sonoshita, M., K. Takaku, N. Sasaki, Y. Sugimoto, F. Ushikubi, S. Narumiya, M. Oshima, and M.M. Taketo. 2001. Acceleration of intestinal polyposis through prostaglandin receptor EP2 in Apc(Delta 716) knockout mice. *Nat. Med.* 7:1048–1051.
 44. Smith, T.J., G.D. Sempowski, H.S. Wang, P.J. Del Vecchio, S.D. Lippe, and R.P. Phipps. 1995. Evidence for cellular heterogeneity in primary cultures of human orbital fibroblasts. *J. Clin. Endocrinol. Metab.* 80:2620–2625.
 45. Goldring S.R., M.L. Stephenson, E. Downie, S.M. Krane, and J.H. Korn. 1990. Heterogeneity in hormone responses and patterns of collagen synthesis in cloned dermal fibroblasts. *J. Clin. Invest.* 85:798–803.
 46. Ko, S.D., R.C. Page, and A.S. Narayanan. 1977. Fibroblast heterogeneity and prostaglandin regulation of subpopulations. *Proc. Natl. Acad. Sci. USA.* 74:3429–3432.
 47. Fukumura, D., F. Yuan, W.L. Monsky, Y. Chen, and R.K. Jain. 1997. Effect of host microenvironment on the microcirculation of human colon adenocarcinoma. *Am. J. Pathol.* 151:679–688.
 48. Gohongi, T., D. Fukumura, Y. Boucher, C.O. Yun, G.A. Soff, C. Compton, T. Todoroki, and R.K. Jain. 1999. Tumor-host interactions in the gallbladder suppress distal angiogenesis and tumor growth: involvement of transforming growth factor beta. *Nat. Med.* 5:1203–1208.
 49. Williams, C.S., M. Tsujii, J. Reese, S.K. Dey, and R.N. DuBois. 2000. Host cyclooxygenase-2 modulates carcinoma growth. *J. Clin. Invest.* 105:1589–1594.
 50. Morikawa, S., P. Baluk, T. Kaidoh, A. Haskell, R.K. Jain, and D.M. McDonald. 2002. Abnormalities in pericytes on blood vessels and endothelial sprouts in tumors. *Am. J. Pathol.* 160:985–1000.
 51. Hossain, M.A., C.M. Bouton, J. Pevsner, and J. Latterra. 2000. Induction of vascular endothelial growth factor in human astrocytes by lead. Involvement of a protein kinase C/activator protein-1 complex-dependent and hypoxia-inducible factor 1-independent signaling pathway. *J. Biol. Chem.* 275:27874–27882.
 52. Park, J.S., L. Qiao, Z.Z. Su, D. Hinman, K. Willoughby, R. McKinstry, A. Yacoub, G.J. Duigou, C.S. Young, S. Grant, et al. 2001. Ionizing radiation modulates vascular endothelial growth factor (VEGF) expression through multiple mitogen activated protein kinase dependent pathways. *Oncogene.* 20: 3266–3280.